2009-01-2034

Vibration Analysis of Powertrain Mounting System with a Combination of Active and Passive Isolators with Spectrally-varying Properties

Jae-Yeol Park and Rajendra Singh
The Ohio State University

ABSTRACT

Most of the prior work on active mounting systems has been conducted in the context of a single degree-of-freedom even though the vehicle powertrain is a six degree-of-freedom isolation system. We seek to overcome this deficiency by proposing a new six degree-of-freedom analytical model of the powertrain system with a combination of active and passive mounts. All stiffness and damping elements contain spectrally-varying properties and we examine powertrain motions when excited by an oscillating torque. Two methods are developed that describe the mount elements via a transfer function (in Laplace domain). New analytical formulations are verified by comparing the frequency responses with numerical results obtained by the direct inversion method (based on Voigt type mount model). Eigensolutions of a spectrally varying mounting system are also predicted by new models. Complex eigenvalue problem formulation with spectrally-varying properties provides a closer match with experimental results than the real eigenvalue formulation with frequency-independent mounts. Given the spectral variance in the mount properties, a simple roll mode decoupling scheme is suggested for the powertrain isolation system. Then, the role of active path is clarified by comparison with no actuator operation. Multi-dimensional motions (especially coupling) are predicted and in particular the effects of active mount parameters such as the orientation angle, location and actuator input are investigated from the motion coupling perspective.

INTRODUCTION

Prior analyses of rigid body isolation systems, including vibration transmissibility, natural frequency placement and motion decoupling studies [1 – 7], assume that the stiffness (*k*) and viscous damping (*c*) properties are constant. However, real-life mount elements inherently (and some even by design) exhibit considerable frequency- and amplitude-dependency, express $k = k(\omega, x)$ and $c = c(\omega, x)$ where ω is the angular frequency (rad/s) and x is the amplitude of excitation [8 – 11]. The rigid body mounting systems are typically modeled in terms of a six degree of freedom (6-DOF) inertial body that is supported by tri-axial isolation elements at 3 or 4 locations along with a rigid foundation [1 – 7]. Yu, Naganathan, and Dukkipati [12], He and Singh [13], and Jeong and Singh [14] have suggested that it is necessary to incorporate the spectrally-varying properties in the engine isolation system models.

Several active or smart engine mounting devices [15 – 19] have been designed to reduce noise and vibration, especially under high dynamic torque conditions. Typical design criteria [1 – 7] include decoupling of powertrain motions and motion control. Motion control is achieved through reduction in resonant peaks, natural frequency placement, reduced vibration transmissibility and increased acoustic comfort. Even though the powertrain (rigid body) is a 6 degree-of-freedom (DOF) isolation system, most of analytical work has been conducted in the context of single-degree-of-freedom systems [15 – 19]. In several cases, high damping solutions have been implemented to control resonance(s) at lower frequencies, and then more compliant mounts have been sought at higher frequencies to minimize the force transmitted in the

The Engineering Meetings Board has approved this paper for publication. It has successfully completed SAE's peer review process under the supervision of the session organizer. This process requires a minimum of three (3) reviews by industry experts.

ISSN 0148-7191

SAE Customer Service: Tel: 877-606-7323 (inside USA and Canada)
Tel: 724-776-4970 (outside USA)
Fax: 724-776-0790
Email: CustomerService@sae.org
SAE Web Address: http://www.sae.org

Printed in USA

SAE International

base; this implies an introduction of frequency-dependent isolators through passive, adaptive or active means. The above-mentioned design may not satisfy the powertrain motion decoupling considerations, and thus the selection of an active mount in the context of a 6-DOF system remains an empirical science. We seek to overcome this deficiency by proposing a new analytical model that will examine a combination of active and passive mounts.

The literature on multi-degree-of-freedom active isolation systems is sparse. For example, Gardonio, Elliott, and Pinnington [20], Kim and Lee [21], and Royston and Singh [22] have limited their analyses to 3-DOF systems (e.g. transverse-axial-pitch motions or pitch-roll-bounce motions). Also, prior researchers have attempted to minimize the forces transmitted into the rigid or compliant foundations without considering the multi-dimensional motion control and coupling issues. In particular, Gardonio, Elliot, and Pinnington [20] and Kim and Lee [21] have suggested that passive and active mount parameters should be properly selected prior to the isolation control problem, especially at the lower frequencies (say up to 50 Hz). This article extends the prior multi-degree-of-freedom active isolators work [20 – 22] by focusing on the eigensolutions, coupling dynamics and motion control issues.

PROBLEM FORMULATION

Figure 1 illustrates a typical 6-DOF rigid body isolation system composed of an inertial body (engine and transmission), a rigid base (chassis), and three or four linear time invariant active and passive mounts such that each isolation element could be arbitrarily placed at any exterior point and oriented in any direction. The dynamic characteristics of isolators are generally represented in terms of the complex-valued cross point dynamic stiffness, $K(\mathrm{j}\omega)$, from non-resonant dynamic tests [8] where j is the imaginary unit. Figure 2 shows sample measurements of $k(\omega)$ and $c(\omega)$ for two example cases (rubber and hydraulic engine mounts). We could embed these or similar $k_i(\omega)$ and $c_i(\omega)$ properties in one or more mount elements of Fig. 1. The governing equations of the mounting system in frequency domain (ω) are as follows, where $\mathbf{q}(\omega)$ is the dynamic displacement vector, and $\mathbf{f}(\omega)$ is the external excitation (force/torque) vector

$$[-\omega^2\mathbf{M} + \mathrm{j}\omega\mathbf{C}(\omega) + \mathbf{K}(\omega)]\mathbf{q}(\omega) = \mathbf{f}(\omega) \qquad (1)$$

Here, $\mathbf{M}$ is the inertial (mass) matrix, and $\mathbf{K}(\omega)$ and $\mathbf{C}(\omega)$ are the stiffness and viscous damping matrices. For an internal combustion powertrain system, the main excitation, $\mathbf{f}(t)$, comes from the pulsating torque that is generated by multi-cylinder engines and it could be either periodic (under steady state) or transient (under start-up or switching conditions). Frequency responses could be numerically calculated by the direct inversion method (designated in this article as Method I), where we could simply use different *k* and *c* values at each frequency (essentially a look-up table scheme). However, Method I in Eq. (1) cannot directly lead to the analytical modal expansion for response predictions and motion coupling analyses. In order to overcome this limitation, Jeong and Singh [14] had formulated several spectral eigenvalue problems and then suggested modal superposition procedures. However, their method is valid for a special class of problems (where the dynamic stiffness is given in a specific form), and their approximation cannot be extended to a more general spectrally-varying vibrating system.

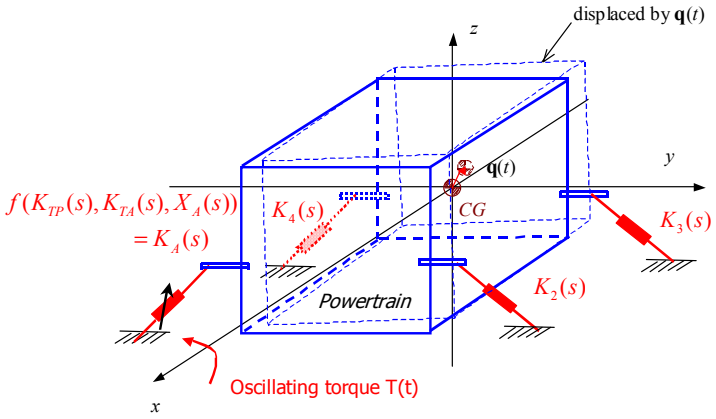

Fig. 1 Multi-degree-of-freedom powertrain isolation system with one active mount and three passive mounts. Each mount is described by tri-axial elements with frequency dependent stiffness $k(\omega)$ and damping $c(\omega)$ properties. Here, $K_i(s)$, *i* = 2, 3, and 4 (= *n*: number of mounts) and $K_A(s)$ are the dynamic stiffness terms of passive and active elements (in a specific direction) respectively.

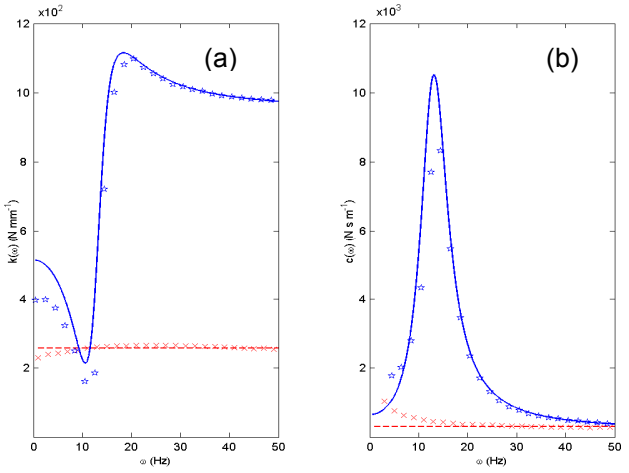

Fig. 2 Mount examples with spectrally-varying stiffness and viscous damping properties. Measured data for rubber and hydraulic mounts are compared, respectively, with transfer function (TF) models given by Eq. (2). (a) Stiffness spectra, $k(\omega) = \mathrm{Re}[K(\mathrm{j}\omega)]$; (b) Viscous damping spectra, $c(\omega) = \mathrm{Im}[K(\mathrm{j}\omega)]/\omega$. Key:

☆, measured data for a hydraulic mount with an excitation amplitude of $x = 1.5$ mm; ×, measured data for a rubber mount; ——, second order TF for the hydraulic mount; — —, zeroth order TF for the rubber mount ($k = 280$ N mm^{-1}, $c = 300$ N s m^{-1}).

The cross-point dynamic stiffness (in Laplace domain *s*) of a typical engine mount at a certain excitation amplitude, under a specific mean load, could be given by the following expression [8]:

$$K_i(s) = \frac{\alpha_b s^b + \cdots + \alpha_3 s^3 + \alpha_2 s^2 + \alpha_1 s + \alpha_0}{\beta_a s^a + \cdots + \beta_2 s^2 + \beta_1 s + \beta_0}. \quad (2)$$

Here, *a* and *b* are the order of denominator and numerator, respectively, and the coefficients, α_k and β_k, are determined by experimental or numerical (analytical) method reflecting the internal fluid structure and rubber material properties. Observe that Eq. (2) matches well with the experimental results of Fig. 2 for hydraulic (with *a* = 2, *b* = 3) and rubber (with *a* = 0, *b* = 1) mounts. Employment of Eq. (2) to the powertrain mounts in Fig. 1 is designated here as Method II. After verification by comparison with experimental and numerical results, this formulation will be used here for vibration and decoupling analysis of powertrain mounting system with combination of active and passive mounts with spectrally-varying properties.

Active and passive mount models that are depicted in Fig. 3. Effective control of powertrain motions is essential over the lower frequency range up to 50 Hz since the rigid body modes significantly dominate and could couple with other vehicle system modes [20, 21]. Actuator displacement in active mounts is adjusted sinusoidally [23, 24] by a displacement actuator, $x_A(t) = X_A e^{j(\omega t + \phi_A)}$ where X_A is active displacement amplitude, ω angular active displacement input frequency, and ϕ_A phase angle with respect to the external torque excitation. Consideration of constant X_A and ϕ_A (at a time) would allow us to make the active mount as analytically tractable in the context of a multi-degree-of-freedom isolation system. Our model will analytically examine the parameters of active and passive mounts (such as stiffness, damping and active input), their locations and orientation angles. Analysis is limited to only the engine torque excitation.

Consider a 6-DOF isolation system consisting of a rigid body (with powertrain mass *m*, and inertia I_{ij}, i and $j = x, y, z$) under an oscillating torque ($T(t)$) and 4 tri-axial mounts which are assumed to be attached to a rigid base. Out of these, one is an active mount (given by subscript *A*) with dynamic stiffness $K_A(s) = f[K_{TP}(s), K_{TA}(s), X_A(s), X(s)]$ in a specific direction where *s* is the Laplace variable, $X(s)$ is the powertrain displacement and $X_A(s)$ is the actuator displacement. The other three are passive devices with dynamic stiffness $K_i(s)$, $i = 2, 3, 4$ in a specific direction. Each mount element (in any direction) is assumed to have frequency-dependent, stiffness $k(\omega)$ and viscous damping $c(\omega)$ properties.

Governing equations in matrix form are as follows, where (*s*) implies the Laplace domain, $\mathbf{q}(s) = [x, y, z, \theta_x, \theta_y, \theta_z]^T(s)$ is the displacement vector, and $\mathbf{f}(s)$ is the external force vector (primarily the torque $T(s)$ excitation),

$$[s^2\mathbf{M} + \mathbf{K}(s)]\mathbf{q}(s) = \mathbf{f}(s), \quad (3)$$

where $\mathbf{M}$ is the mass matrix (powertrain mass and inertia), and $\mathbf{K}(s)$ is the stiffness matrix that includes the transfer function (dynamic stiffness) models of active and passive mounts. Passive mounts are modeled as shown in Fig. 3(a) in terms of the cross point stiffness [8, 13] $K_T(s) = F_T(s)/X(s)$. Here, $K_T(s)$ could be either analytically available from a fluid mount model [8] or experimentally measured by a non-resonance mount test [13, 25]. This type of transfer function model is valid in the lower frequency range (say up to 50 Hz).

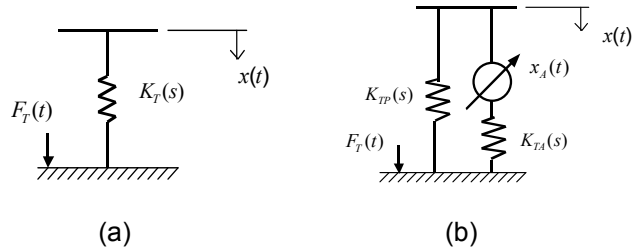

(a) (b)

Fig. 3 Passive and active engine mounts given displacement input $x(t)$. (a) Passive mount; (b) Active mount with piston displacement type input ($x_A(t)$). In both cases, force transmitted to the rigid base is $F_T(t)$. Stiffness terms are given in the Laplace domain.

The chief objective of this article is to investigate the complex eigensolutions and frequency responses of the powertrain system of Fig. 1, when excited by an oscillating torque, with one active mount and 3 passive mounts. The active mount model of Fig. 3(b) is first formulated for fluid piston type active device such as a hydraulic engine mount [1, 3 - 5]. Our method will be validated by comparing analytical predictions in frequency domain with the direct inversion (numerical) method where we could simply use different k and c values at each frequency. The second objective is to examine multi-directional motion control and vibration isolation issues in the context of a multi-degree-of-freedom mounting system.

Gennesseaux [26] examined four active isolation schemes and concluded that an actuator structure in

parallel with a rubber element is the most preferred design, as the active actuator should be designed to generate only the dynamic force, and the static force should be provided by the rubber element. Based on this concept, a new analytical model for active mounts with actuator displacement input is proposed in Fig. 3(b). Since this work is limited to the lower frequency regime, the cross point transfer function ($K_T(s)$) concept is also applied to represent the dynamic property of an active mount. In this model, the force transmitted into the rigid base ($F_T(s)$), consists of a passive force ($F_{TP}(s)$) and an active force ($F_{TA}(s)$):

$$F_T(s) = F_{TP}(s) + F_{TA}(s). \quad (4)$$

The individual transfer functions, $K_{TP}(s)$ and $K_{TA}(s)$, of the passive (primary) and active (secondary) paths are defined by the following:

$$K_{TP}(s) = \frac{F_{TP}(s)}{X(s)} \quad \text{and} \quad K_{TA}(s) = \frac{F_{TA}(s)}{X_A(s)}. \quad (5a, b)$$

Here, $X(s)$ is the powertrain displacement's principal direction component of the active mount, and $X_A(s)$ is the actuator displacement in Laplace domain. For a single-degree-of-freedom isolation system of Fig. 4, the governing equation is:

$$[ms^2 + K_{TP}(s)]X(s) = F(s) - K_{TA}(s)X_A(s). \quad (6)$$

Here, the active force, $F_{TA}(s) = K_{TA}(s)X_A(s)$, can be viewed as an "additional external" excitation since it acts independent of $X(s)$. Therefore, the eigensolutions and passive dynamics are governed by the passive path ($K_{TP}(s)$). While an adaptive mount is usually designed to have at least two passive transfer functions depending on designated operating conditions [25], only one passive transfer function is assigned to an active mount. Therefore, detailed dynamic analysis of the passive element in an active mounting system is crucial.

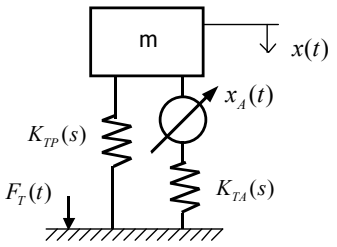

Fig. 4 Single-degree-of-freedom system with an active mount.

Two active mount concepts, where the actuator element is in parallel with the passive rubber element, will be examined. First, consider an active hydraulic device as shown in Fig. 5. The active mount consists of three control volumes (upper and lower chambers are designated by *#1* and *#2*, respectively, and the inertia track is represented by *#i*). The momentum equation for rubber mass, m_r, is:

$$m_r\ddot{x}(t) = F(t) - k_r x(t) - c_r\dot{x}(t) - A_r p_1(t). \quad (7)$$

The continuity equations for the lower and upper chambers are:

$$A_r\dot{x}(t) - q_i(t) = C_1\dot{p}_1(t) + A_A\dot{x}_A(t), \quad (8)$$

$$q_i(t) = C_2\dot{p}_2(t). \quad (9)$$

The momentum equation for the inertia track is:

$$p_1(t) - p_2(t) = I_i\dot{q}_i(t) + R_i q_i(t). \quad (10)$$

Since $F(t) = F_T(t)\ (= F_{TP}(t) + F_{TA}(t))$ in the lower frequency range [8], the transfer functions for this active mount are derived from Eqs. (7) - (10) as follows:

$$\begin{cases} K_{TP}(s) = \dfrac{F_{TP}(s)}{X(s)} = m_r s^2 + c_r s + k_r + \dfrac{\alpha_2 s^2 + \alpha_1 s + \alpha_0}{\beta_2 s^2 + \beta_1 R_i s + \beta_0} A_r \\ K_{TA}(s) = \dfrac{F_{TA}(s)}{X_A(s)} = -\dfrac{\alpha_2 s^2 + \alpha_1 s + \alpha_0}{\beta_2 s^2 + \beta_1 R_i s + \beta_0} A_A \end{cases}, \quad (11a, b)$$

$$\alpha_2 = C_2 A_r I_i, \quad \alpha_1 = C_2 A_r R_i, \quad \alpha_0 = A_r^2, \quad (11c\text{-}e)$$

$$\beta_2 = I_i C_1 C_2, \quad \beta_1 = C_1 C_2 R_i, \quad \beta_0 = C_1 + C_2. \quad (11f\text{-}h)$$

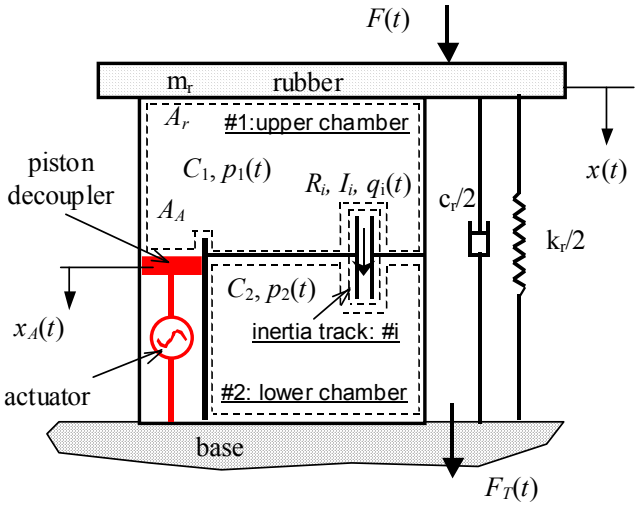

Fig. 5 Schematic of an active engine mount based on hydraulic mount. Here, C_1 and C_2 are the compliances of upper and lower chambers, $p_1(t)$ and $p_2(t)$ are the chamber pressures, R_i, I_i, and $q_i(t)$ are the fluid resistance, inertance, and flow rate in the inertia track, A_r is the equivalent piston area of rubber, A_A is the actuator piston area, and k_r and c_r are the rubber stiffness and viscous damping terms (Voigt model assumed).

MULTI-DEGREE-OF-FREEDOM ISOLATION SYSTEM WITH ACTIVE AND PASSIVE MOUNTS

We consider the powertrain isolation system (Fig. 1) with one or two active mounts and two or three rubber mounts. The following three coordinate systems are used: inertial reference coordinates $(\mathrm{XYZ})_g$ fixed at the ground with its origin at the static equilibrium (at the center of gravity, CG), along with local mount coordinates $(\mathrm{XYZ})_{\mathrm{m},i}$ which are parallel to $(\mathrm{XYZ})_{\mathrm{g}}$ and principal mount coordinates $(\mathrm{XYZ})_{\mathrm{mp},i}$ whose principal axes are not parallel to $(\mathrm{XYZ})_{\mathrm{g}}$, where subscript i $(=1,2,\cdots,n)$ is the mount index and n is the number of mounts. Passive rubber mounts formulated by $K_i(s)=k_i+c_i s$ are described by three tri-axial spring and viscous (or structural) damping elements; the stiffness values are assumed to be constant and insensitive to the excitation amplitude. Conversely, active mounts are described by $K_{TP}(s)$ and $K_{TA}(s)$ as developed in the previous section. Only the torque excitation is considered in this article even though any excitation forces can be applied to the rigid powertrain. The displacements of the time-invariant inertial body (of dimension six) are assumed to be small and the displacement vector $\mathbf{q}(t)=[x\ y\ z\ \theta_x\ \theta_y\ \theta_z]^{\mathrm{T}}(t)$ is expressed by the translational and angular displacements of the center of gravity (CG). The governing equations are formulated in matrix form, as shown below, where $\dot{\mathbf{q}}(t)$ and $\ddot{\mathbf{q}}(t)$ are the velocity, and acceleration vectors, respectively:

$$\mathbf{M}\ddot{\mathbf{q}}(t)+\mathbf{C}\dot{\mathbf{q}}(t)+\mathbf{K}\mathbf{q}(t)=\mathbf{f}(t)+\mathbf{f}_{\mathrm{A}}(t). \qquad (12)$$

Here, $\mathbf{M}$ is inertial (mass) matrix, $\mathbf{K}$ is the stiffness matrix, $\mathbf{C}$ is the viscous damping matrix, and $\mathbf{f}(t)$ is the external excitation (force/torque) vector. Here, $\mathbf{f}_{\mathrm{A}}(t)$ is the reaction force generated by the active mounts; rewrite it as $\mathbf{f}_{\mathrm{A}}(t)=\mathbf{f}_{\mathrm{TP}}(t)+\mathbf{f}_{\mathrm{TA}}(t)$, where $\mathbf{f}_{\mathrm{TP}}(t)$ and $\mathbf{f}_{\mathrm{TA}}(t)$ are the forces from the passive and active paths respectively. Equation (12) becomes:

$$\mathbf{M}\ddot{\mathbf{q}}(t)+\mathbf{C}\dot{\mathbf{q}}(t)+\mathbf{K}\mathbf{q}(t)=\mathbf{f}(t)+\mathbf{f}_{\mathrm{TP}}(t)+\mathbf{f}_{\mathrm{TA}}(t). \qquad (13)$$

The reaction forces, $\mathbf{f}_{\mathrm{TP}}(t)$ and $\mathbf{f}_{\mathrm{TA}}(t)$, are the sum of forces generated by each active mount element and they are expressed as follows where N_{A} is the number of active mounts:

$$\mathbf{f}_{\mathrm{TP}}(t)=\sum_{k=1}^{N_{\mathrm{A}}}\mathbf{f}_{\mathrm{TP},k}(t) \quad \text{and} \quad \mathbf{f}_{\mathrm{TA}}(t)=\sum_{k=1}^{N_{\mathrm{A}}}\mathbf{f}_{\mathrm{TA},k}(t). \qquad (14)$$

Utilize the transfer function models of Eq. (5) to represent the passive and active paths of N_{A} active mounts as follows:

$$K_{TP,k}(s)=\frac{F_{TP,k}(s)}{X_{TP,k}(s)}=\frac{\mathcal{L}\left[f_{TP,k}(t)\right]}{\mathcal{L}\left[x_{TP,k}(t)\right]},\ k=1,\cdots,N_{\mathrm{A}}, \qquad (15a)$$

$$K_{TA,k}(s)=\frac{F_{TA,k}(s)}{X_{A,k}(s)}=\frac{\mathcal{L}\left[f_{TA,k}(t)\right]}{\mathcal{L}\left[x_{A,k}(t)\right]},\ k=1,\cdots,N_{\mathrm{A}}. \qquad (15b)$$

Here, $\mathcal{L}$ is the Laplace transform. Note that $f_{TP,k}(t)$ and $f_{TA,k}(t)$ are passive and active path forces, respectively, in a specific direction of an active mount component, while $x_{TP,k}(t)$ and $x_{A,k}(t)$ are inertial body displacement in the active mount orientation direction and active input displacement in time domain. The local mount reaction forces, $f_{TP,k}(t)$ and $f_{TA,k}(t)$, are represented in the global $(\mathrm{XYZ})_g$ coordinates in terms of the mount parameters and their orientation angles and locations; the inertial body displacement, $x_{TP,k}(t)$, is found based on the kinematics of isolation system. The resulting deflection, $\mathbf{q}_{mi,t}(t)$, at each mount is as follows, based on the rigid foundation assumption:

$$\mathbf{q}_{mi,t}(t)=\begin{bmatrix}\mathbf{I} & \mathbf{L}_{mi}\end{bmatrix}\mathbf{q}(t), \qquad (16)$$

$$\mathbf{L}_{mi}=\begin{bmatrix}0 & r_{zi} & -r_{yi}\\ & 0 & r_{xi}\\ \text{skew sym.} & & 0\end{bmatrix} \qquad (17)$$

Using the Euler angles as given by $(\theta_i,\varphi_i,\phi_i)$ for i-th mount, the rotational matrix, $\mathbf{\Theta}_{g,mi}$ is found by rotating about $(\mathrm{XYZ})_g$ axes in the sequence of X, Y, and Z [3]. Reaction force in the i-th mount in the global coordinate system is obtained by a transformation from the local mount coordinates, and the resulting reaction force is:

$$\mathbf{f}_{\mathrm{g,m}i}(t)=\begin{bmatrix}\mathbf{f}_{\mathrm{g,m}i,\mathrm{t}}(t)\\ \mathbf{f}_{\mathrm{g,m}i,\theta}(t)\end{bmatrix}=\begin{bmatrix}\mathbf{f}_{\mathrm{m}i,\mathrm{t}}(t)\\ \mathbf{r}_{\mathrm{m}i}\times\mathbf{f}_{\mathrm{m}i,t}(t)\end{bmatrix}=\begin{bmatrix}\mathbf{I}\\ \mathbf{L}_{mi}^{\mathrm{T}}\end{bmatrix}\mathbf{f}_{mi,t}(t). \qquad (18)$$

Since $\mathbf{f}_{mi,t}(t)=\mathbf{\Theta}_{\mathrm{g,m}i}\mathbf{f}_{mpi,t}(t)$, Eq. (18) becomes:

$$\mathbf{f}_{\mathrm{g,m}i}(t)=\begin{bmatrix}\mathbf{I}\\ \mathbf{L}_{mi}^{\mathrm{T}}\end{bmatrix}\mathbf{\Theta}_{\mathrm{g,m}i}\mathbf{f}_{\mathrm{mp}i,t}(t). \qquad (19)$$

Based on the fact that the transmitted (output reaction) forces, $f_{TP,k}(t)$ and $f_{TA,k}(t)$, through active mount are described in the $(\mathrm{XYZ})_{\mathrm{mp}i}$ coordinates as $\mathbf{f}_{TP,k-\mathrm{mp}i}(t)=\begin{bmatrix}f_{TP,k}(t) & 0 & 0\end{bmatrix}^{\mathrm{T}}$ and $\mathbf{f}_{TA,k-\mathrm{mp}i}(t)=\begin{bmatrix}f_{TA,k}(t) & 0 & 0\end{bmatrix}^{\mathrm{T}}$, their transformations ($\mathbf{f}_{TP,k}(t)$ and $\mathbf{f}_{TA,k}(t)$) to the global coordinate system are expressed using Eq. (19) as follows:

$$\mathbf{f}_{TP,k}(t)=\mathbf{f}_{TP,k-g,\mathrm{m}i}(t)=\begin{bmatrix}\mathbf{I}\\ \mathbf{L}_{\mathrm{m}i}^{\mathrm{T}}\end{bmatrix}\mathbf{\Theta}_{\mathrm{g,m}i}\begin{bmatrix}f_{TP,k}(t)\\ 0\\ 0\end{bmatrix}, \qquad (20a)$$

$$\mathbf{f}_{TA,k}(t)=\mathbf{f}_{TA,k-g,\mathrm{m}i}(t)=\begin{bmatrix}\mathbf{I}\\ \mathbf{L}_{\mathrm{m}i}^{\mathrm{T}}\end{bmatrix}\mathbf{\Theta}_{\mathrm{g,m}i}\begin{bmatrix}f_{TA,k}(t)\\ 0\\ 0\end{bmatrix}, \qquad (20b)$$

where, $f_{TA,k}(t)=\mathcal{L}^{-1}\left[K_{TA,k}(s)X_{A,k}(s)\right]$, $k=1,\cdots,N_{\mathrm{A}}$. Along with $\mathbf{q}_{mpi,\theta}(t)=\mathbf{\Theta}_{\mathrm{g,m}i}^{\mathrm{T}}\mathbf{q}_{\theta}(t)$, the displacement of the

i-th mount with respect to the principal mount coordinates, $(\mathrm{XYZ})_{\mathrm{mp}i}$, is expressed as follows:

$$\mathbf{q}_{\mathrm{mp}i}(t)=\begin{bmatrix}\mathbf{q}_{\mathrm{mp}i,\mathrm{t}}(t)\\ \mathbf{q}_{\mathrm{mp}i,\theta}(t)\end{bmatrix}=\mathbf{\Theta}^{\mathrm{T}}_{\mathrm{g,m}i}\begin{bmatrix}\mathbf{I} & \mathbf{L}_{\mathrm{m}i}\\ \mathbf{0} & \mathbf{I}\end{bmatrix}\mathbf{q}(t)\,. \tag{21}$$

Since the inertial displacement, $x_{TP,k}(t)$, to an active mount from rigid body motion ($\mathbf{q}(t)$) is set to be one of the principal directions of *i*-th mount component, $x_{TP,k}(t)$ is obtained by finding a corresponding vector element in $\mathbf{q}_{\mathrm{mp},i}(t)$ of Eq. (21) as follows:

$$x_{TP,k}(t)=\mathbf{q}_{\mathrm{mp}i,\nu}(t)\,,\quad \nu=x \text{ or } y \text{ or } z\,. \tag{22}$$

The resulting inertial displacement in the direction of the active mount component is now completely described in terms of the orientation angle, its location, and rigid body motion without introducing an additional variable for itself. We apply the inverse Laplace transformation to convert Eq. (15) to time domain formulation and obtain the equations as:

$$\mathbf{a}(t)=\mathbf{b}_{TP}(t)\,, \tag{23}$$

where, by assuming that a typical transfer function ($K_{TP,k}(s)$) is assumed to be represented as $K_{TP,k}(s)=(\alpha_{2,k}s^2+\alpha_{1,k}s+\alpha_{0,k})/(\beta_{2,k}s^2+\beta_{1,k}s+\beta_{0,k})$, based on the fact that an active hydraulic mount is modeled in Eq. (11) when m_r and c_r are negligible in lower frequency range [8],

$$\mathbf{a}(t)=\left[a_1,\cdots,a_{N_A}\right]^{\mathrm{T}}(t)\,,$$

$$a_k(t)=\mathcal{L}^{-1}\left[(\alpha_{2,k}s^2+\alpha_{1,k}s+\alpha_{0,k})X_{TP,k}(s)\right],\quad k=1,\cdots,N_{\mathrm{A}} \tag{24a}$$

$$\mathbf{b}_{TP}(t)=\left[b_{TP,1},\cdots,b_{TP,N_A}\right]^{\mathrm{T}}(t)\,,$$

$$b_{TP,k}(t)=\mathcal{L}^{-1}\left[(\beta_{2,k}s^2+\beta_{1,k}s+\beta_{0,k})F_{TP,k}(s)\right],\quad k=1,\cdots,N_{\mathrm{A}}\,. \tag{24b}$$

Note that $X_{TP,k}(s)$ in Eq. (24) is:

$$X_{TP,k}(s)=\left\{\mathbf{\Theta}^{\mathrm{T}}_{\mathrm{g,m}i}\begin{bmatrix}\mathbf{I} & \mathbf{L}_{\mathrm{m}i}\\ \mathbf{0} & \mathbf{I}\end{bmatrix}\mathbf{Q}(s)\right\}_X\,. \tag{25}$$

For an asymmetric mounting system, Eqs. (13) and (23) are expanded using the powertrain system kinematics developed above and the governing equations with active and passive mounts are represented in an extended form as follows:

$$m\ddot{x}(t)+\mathbf{c}^T_{mx}\dot{\mathbf{q}}(t)+\mathbf{k}^T_{mx}\mathbf{q}(t)=(\mathbf{f})_x+(\mathbf{f}_{TA})_x+f_{rx}(f_{TP,1},\cdots,\mathrm{f}_{TP,N_A})\,, \tag{26a}$$

$$m\ddot{y}(t)+\mathbf{c}^T_{my}\dot{\mathbf{q}}(t)+\mathbf{k}^T_{my}\mathbf{q}(t)=(\mathbf{f})_y+(\mathbf{f}_{TA})_y+f_{ry}(f_{TP,1},\cdots,\mathrm{f}_{TP,N_A})\,, \tag{26b}$$

$$m\ddot{z}(t)+\mathbf{c}^T_{mz}\dot{\mathbf{q}}(t)+\mathbf{k}^T_{mz}\mathbf{q}(t)=(\mathbf{f})_z+(\mathbf{f}_{TA})_z+f_{rz}(f_{TP,1},\cdots,\mathrm{f}_{TP,N_A})\,, \tag{26c}$$

$$I_{xx}\ddot{\theta}_x(t)+I_{xy}\ddot{\theta}_y(t)+I_{xz}\ddot{\theta}_z(t)+\mathbf{c}^T_{m\theta_x}\dot{\mathbf{q}}(t)+\mathbf{k}^T_{m\theta_x}\mathbf{q}(t)=(\mathbf{f})_{\theta_x}+(\mathbf{f}_{TA})_{\theta_x}+M_{r\theta_x}(f_{TP,1},\cdots,\mathrm{f}_{TP,N_A})\,, \tag{26d}$$

$$I_{xy}\ddot{\theta}_x(t)+I_{yy}\ddot{\theta}_y(t)+I_{yz}\ddot{\theta}_z(t)+\mathbf{c}^T_{m\theta_y}\dot{\mathbf{q}}(t)+\mathbf{k}^T_{m\theta_y}\mathbf{q}(t)=(\mathbf{f})_{\theta_y}+(\mathbf{f}_{TA})_{\theta_y}+M_{r\theta_y}(f_{TP,1},\cdots,\mathrm{f}_{TP,N_A})\,, \tag{26e}$$

$$I_{xz}\ddot{\theta}_x(t)+I_{yz}\ddot{\theta}_y(t)+I_{zz}\ddot{\theta}_z(t)+\mathbf{c}^T_{m\theta_z}\dot{\mathbf{q}}(t)+\mathbf{k}^T_{m\theta_z}\mathbf{q}(t)=(\mathbf{f})_{\theta_z}+(\mathbf{f}_{TA})_{\theta_z}+M_{r\theta_z}(f_{TP,1},\cdots,\mathrm{f}_{TP,N_A})\,, \tag{26f}$$

$$\mathrm{h}_k(x^{(b)}_{fd,k}(t),\cdots,x_{fd,k}(t))=\mathrm{b}_k(f^{(2)}_{TP,1},\cdots,f_{TP,1},\ \cdots,f^{(2)}_{TP,N_A},\cdots,f_{TP,N_A})\quad k=1,2,\cdots,N_{\mathrm{A}}\,. \tag{26g}$$

Combining Eqs. (26a – g) and assuming zero initial conditions in the inverse Laplace transform in Eq. (26g), we assemble the following "extended" governing equations (in matrix form) for the mounting system with active mounts:

$$\mathbf{M}_{\mathrm{e}}\ddot{\mathbf{q}}_e(t)+\mathbf{C}_{\mathrm{e}}\dot{\mathbf{q}}_{\mathrm{e}}(t)+\mathbf{K}_{\mathrm{e}}\mathbf{q}_{\mathrm{e}}(t)=\mathbf{f}_{\mathrm{e}}(t)\,. \tag{27}$$

Here, $\mathbf{M}_e$, $\mathbf{C}_e$, and $\mathbf{K}_e$ are extended system matrices as defined below:

$$\mathbf{M}_{\mathrm{e}}=\begin{bmatrix}\mathbf{M} & \mathbf{0}\\ \mathbf{0} & \mathbf{M}_{\mathrm{TP}}\end{bmatrix},\ \mathbf{C}_{\mathrm{e}}=\begin{bmatrix}\mathbf{C} & \mathbf{C}_{1,TP}\\ \mathbf{C}_{2,TP} & \mathbf{C}_{3,TP}\end{bmatrix},\text{ and}$$

$$\mathbf{K}_{\mathrm{e}}=\begin{bmatrix}\mathbf{K} & \mathbf{K}_{1,TP}\\ \mathbf{K}_{2,TP} & \mathbf{K}_{3,TP}\end{bmatrix}.$$

Extended excitation and displacement vectors are

$$\mathbf{f}_{\mathrm{e}}(t)=\left[\mathbf{f}^{\mathrm{T}}(t)+\mathbf{f}^{\mathrm{T}}_{TA}(t)\quad \boldsymbol{\sigma}^{\mathrm{T}}_{\mathrm{TP}}(t)\right]^{\mathrm{T}}$$

$$=\left[\mathbf{f}^{\mathrm{T}}(t)+\mathbf{f}^{\mathrm{T}}_{TA}(t)\quad \sigma_{TP,1}(t)\quad\cdots\quad\sigma_{TP,N_{\mathrm{A}}}(t)\right]^{\mathrm{T}},$$

$$\mathbf{q}_{\mathrm{e}}(t)=\left[\mathbf{q}^{\mathrm{T}}(t)\quad \mathbf{f}^{T}_{\mathrm{TP}}(t)\right]^{\mathrm{T}}$$

where, $\mathbf{f}_{\mathrm{TP}}(t)=\left[f_{TP,1}(t)\quad\cdots\quad f_{TP,N_A}(t)\right]^{\mathrm{T}}$.

Since the reaction forces, $f_{TP,k}(t)$, in active mounts depend on the inertial displacement, $x_{TP,k}(t)$, they are embedded as additional elements in the extended displacement vector, $\mathbf{q}_{\mathrm{e}}(t)$. They mainly act as additional force elements in both expanded displacement and external force vectors. Observe that matrices, $\mathbf{M}_{\mathrm{e}}$, $\mathbf{C}_{\mathrm{e}}$, and $\mathbf{K}_{\mathrm{e}}$, are spectrally-invariant even though they are not symmetric due to an asymmetry in the expanded formulation. We employ this active isolation system model for further analyses.

To apply the complex modal method to a non-conservative discrete system, Eq. (27) is cast in the state-space, first order system form [3] as:

$$\mathbf{A}\dot{\mathbf{p}}(t)+\mathbf{B}\mathbf{p}(t)=\mathbf{g}(t)\,, \tag{28}$$

where the state vector $\mathbf{p}(t)$ and excitation vector $\mathbf{g}(t)$ are defined as:

$$\mathbf{p}(t)=\begin{bmatrix}\dot{\mathbf{q}}_{\mathrm{e}}(t)\\ \mathbf{q}_{\mathrm{e}}(t)\end{bmatrix},\ \mathbf{g}(t)=\begin{bmatrix}\mathbf{f}_{\mathrm{e}}(t)\\ \mathbf{0}\end{bmatrix}, \tag{29a, b}$$

and system matrices $\mathbf{A}$ and $\mathbf{B}$ are defined as:

$$\mathbf{A}=\begin{bmatrix}\mathbf{M}_{\mathrm{e}} & \mathbf{0}\\ \mathbf{0} & -\mathbf{K}_{\mathrm{e}}\end{bmatrix},\ \mathbf{B}=\begin{bmatrix}\mathbf{C}_{\mathrm{e}} & \mathbf{K}_{\mathrm{e}}\\ \mathbf{K}_{\mathrm{e}} & \mathbf{0}\end{bmatrix}. \tag{30a, b}$$

The complex eigenvalue problem associated with Eq. (28) is

$$\lambda_r \mathbf{A}\mathbf{U}_r + \mathbf{B}\mathbf{U}_r = \mathbf{0}, \tag{31}$$

where $\lambda_r \in \mathrm{C}$ ($r = 1, 2, 3, \cdots, 2(N+N_\mathrm{A})$) is the *r*-th complex-valued eigenvalue (includes both real and imaginary parts due to viscous damping) and $\mathbf{U}_r$ is the *r*-th state-space complex-valued eigenvector. The complex eigenvectors $\mathbf{U}_r$ are $\mathbf{U}_r = [\lambda_r \mathbf{u}_r \quad \mathbf{u}_r]^\mathrm{T}$, where $\mathbf{u}_r$ is the configuration (physical) space eigenvector that satisfies the following eigenvalue problem: $[\lambda_r^2 \mathbf{M}_\mathrm{e} + \lambda_r \mathbf{C}_\mathrm{e} + \mathbf{K}_\mathrm{e}]\mathbf{u}_r = \mathbf{0}$. To develop an expansion theorem for asymmetric eigensystem (non-self-adjoint discrete system), an additional eigenvalue problem for the adjoint eigensystem must be defined as:

$$\lambda_r \mathbf{A}^\mathrm{T}\mathbf{V}_r + \mathbf{B}^\mathrm{T}\mathbf{V}_r = \mathbf{0}, \tag{32}$$

in which $\mathbf{V}_r$ is the *r*-th eigenvector of the adjoint system (in state space) that is in the form of $\mathbf{V}_r = [\lambda_r \mathbf{v}_r \quad \mathbf{v}_r]^\mathrm{T}$. Based on the bi-orthogonal property: $\mathbf{V}_r^\mathrm{T}\mathbf{A}\mathbf{U}_s = \delta_{rs}$, $\mathbf{V}_r^\mathrm{T}\mathbf{B}\mathbf{U}_s = -\lambda_r \delta_{rs}$, $r, s = 1, 2, 3, \cdots, 2(N+N_\mathrm{A})$ where δ_{rs} is the Kroneker delta function, the modal expansion theorem is now applicable to our active powertrain mounting system.

Assuming $\mathbf{g}(t) = \mathbf{G}\mathrm{e}^{\mathrm{j}\omega t}$, the harmonic response is as follows:

$$\mathbf{p}(t) = \mathbf{U}^\mathrm{T}(\mathrm{j}\omega\mathbf{I} - \mathbf{\Lambda})\mathbf{V}\mathbf{G}\mathrm{e}^{\mathrm{j}\omega t}, \tag{33}$$

where,

$$\mathbf{U} = \begin{bmatrix} \mathbf{u}_1 & \mathbf{u}_2 & \cdots & \mathbf{u}_{2(N+N_\mathrm{A})-1} & \mathbf{u}_{2(N+N_\mathrm{A})} \end{bmatrix},$$

$$\mathbf{V} = \begin{bmatrix} \mathbf{v}_1 & \mathbf{v}_2 & \cdots & \mathbf{v}_{2(N+N_\mathrm{A})-1} & \mathbf{v}_{2(N+N_\mathrm{A})} \end{bmatrix},$$

$$\mathbf{\Lambda} = \mathrm{diag}\left(\begin{bmatrix} \lambda_1 & \lambda_2 & \cdots & \lambda_{2(N+N_\mathrm{A})-1} & \lambda_{2(N+N_\mathrm{A})} \end{bmatrix}\right).$$

The frequency response functions given harmonic torque excitation (with unity amplitude) are calculated using the modal expansion theorem and compared with those computed using method I.

RESULTS AND DISSCUSSION

In the focalized mounting system as shown in Fig. 6, an inertial coordinate system is chosen to be the same as the principal coordinate system and elastic center lies on one of the principal axes, say the x axis. Oscillating torque is assumed to be in the direction. It is the most desired case for the mounting system in terms of elastic axis focalization or torque roll axis decoupling design since it would yield a complete decoupling given the torque excitation. Based on the proposed system model and complex eigenvalue formulation, eigensolutions for a focalized active mounting system of Figs. 1 and 6 are first analytically examined given the following powertrain parameters: Mass $m = 100.5\ \mathrm{kg}$; moment of inertia $(\mathrm{kg\,m^2})$ $I_{XX} = 1.65$, $I_{YY} = 2.43$, $I_{ZZ} = 2.54$; inertia product $(\mathrm{kg\,m^2})$ $I_{XY} = I_{XZ} = I_{YZ} = 0$. Properties and locations of the rubber mounts are: stiffness $k_a = 280\ \mathrm{N\,mm^{-1}}$; stiffness rate ratio $L_k (= k_a / k_b) = 2.5$; damping $c_a = 30\ \mathrm{N\,s\,m^{-1}}$; damping rate ratio $L_c (= c_a / c_b) = 2.5$; mount orientation $\phi = 0°$; mount locations in the x-direction $r_{x,1} = r_{x,2} = 318\ \mathrm{mm}$, $r_{x,3} = r_{x,4} = -318\ \mathrm{mm}$; mount locations in the y-direction $r_{y,1} = r_{y,3} = -198\ \mathrm{mm}$, $r_{y,2} = r_{y,4} = 198\ \mathrm{mm}$; and mount locations in the z-direction $r_{z,1} = r_{z,2} = r_{z,3} = r_{z,4} = -94\ \mathrm{mm}$. The active mount of Fig. 5 is now placed at location #1 and parameters of Eq. (14) are given as follows [1] when m_r and c_r are negligible [8] over lower frequency range (up to 50 Hz): $k_r = 127.4\ \mathrm{N\,mm^{-1}}$, $A_r = 4123 \times 10^{-6}\ \mathrm{m^2}$, $A_d = 1662 \times 10^{-6}\ \mathrm{m^2}$, $\alpha_2 = 16.2$, $\alpha_1 = 103$, $\alpha_0 = 2590$, $\beta_2 = 2.12 \times 10^{-7}$, $\beta_1 = 1.36 \times 10^{-6}$, and $\beta_0 = 8.18 \times 10^{-4}$. Eigenvalues are compared in Table 1, for passive and active mounts. One additional eigenvalue with a high damping ratio exists in the active mounting system (due to a pole in the passive path), while the isolation system with purely passive (and frequency-independent) mounts has only six eigenvalues. Observe that the resonant frequencies would differ from those obtained when we employ passive rubber mounts (with $K(s) = k + cs$ model). Note that *z* and θ_y modes are significantly coupled with θ_x due to the active mount, and the corresponding resonances show large changes from those for the passive mounting system alone. Since the eigen-structure of an active isolation system is determined by the internal passive path ($K_{TP}(s)$), both passive and active paths must be carefully identified before any parametric design studies can be carried out.

For the sake of illustration, we examine the modes of a V6 diesel engine isolation system [6]. The inertia property is close to be symmetric with respect to crankshaft axis and four mounts are also placed in nearly symmetric locations. Real and complex eigensolutions are calculated and compared with measured natural frequencies in Fig. 7. This analysis suggests that the measured natural frequency at 12.47 Hz corresponds to the sixth (and not the fifth) mode. Better agreement with measured data is achieved only when the complex eigensolution method (with consideration of mount damping) is applied. This implies that the complex eigensolution method should be utilized to analyze the real-life engine mounting systems.

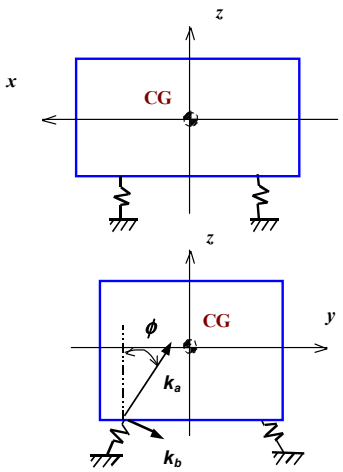

Fig. 6 Focalized powertrain mounting system (6-DOF). Here, k_a is the principal compressive stiffness and k_b is the principal shear stiffness.

Table 1 Comparison of eigenvalues for a powertrain mounting system (Fig. 6) with three passive mounts and one active isolator (Fig. 5)

$K(s)=k+cs$: Passive rubber mount			$K(s)=K_A(s)$: Active mount		
Dominant mode(s)	ω_r (Hz)	ζ (%)	Dominant mode(s)	ω_r (Hz)	ζ (%)
-	-	-	Mount mode	6.2	7.33
y (θ_x)	10.1	0.42	y (θ_x)	10.2	0.41
x	10.4	0.38	x	10.5	0.43
z	16.8	1.83	z, (θ_x,θ_y)	18.0	0.62
θ_z	25.0	0.84	θ_z	25.0	0.84
θ_x	27.3	2.76	θ_x	28.8	0.83
θ_y	34.9	3.73	θ_y , (θ_x)	38.2	0.69

Key: ω_r = natural frequency; ζ = damping ratio.

Fig. 8 shows frequency responses for three translations and three rotations; observe that the analytical model using Method II exactly matches with numerical (direct inversion method) results using Method I. The effect of harmonic active displacement ($x_A(t)=X_A e^{j(\omega t+\phi_A)}$) on the focalized mounting system motions is examined next. Figure 9 compares the frequency responses for three different active displacement inputs given $T(t)=T_{eng}e^{j\omega t}$ with $T_{eng}=100$ N m. Observe that the roll motion (θ_X) is significantly reduced in overall frequency range when the actuator displacement is out of phase with the torque excitation while it is amplified by an in-phase actuator input. This indicates that the active mount could act as a roll control mount even though some coupled motions in other directions are seen. Modal characteristics do not change with active force operation (as expected) since

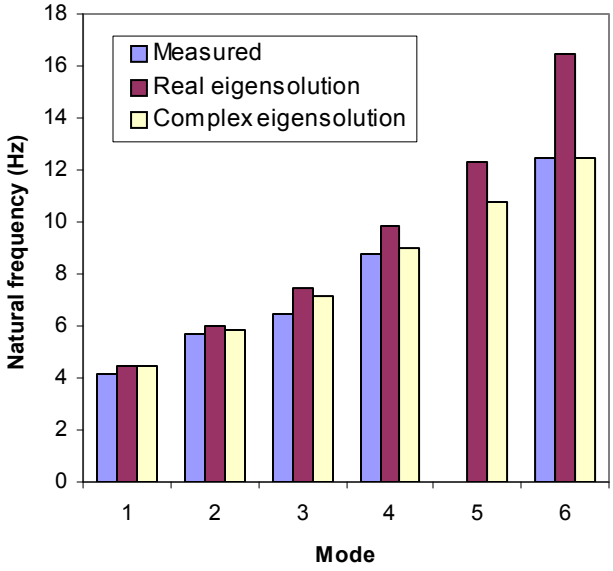

Fig. 7 Comparison of calculated (using both real and complex eigensolution methods) and measured [6] natural frequencies for a V6 diesel engine

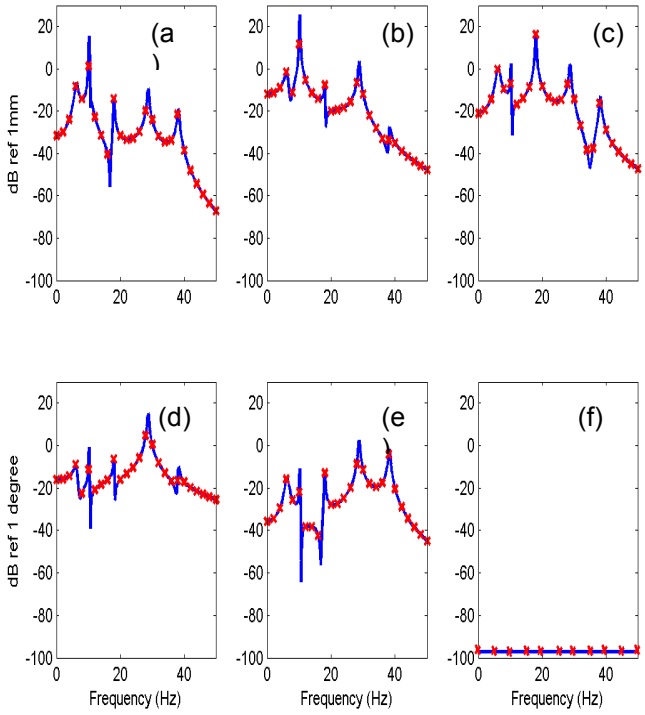

Fig. 8 Frequency response of an active powertrain mounting system of Fig. 6 given harmonic torque with 100 Nm amplitude. One active mount of Fig. 5 is placed at location #1 and the rest are passive mounts. (a) $X(\omega)$; (b) $Y(\omega)$; (c) $Z(\omega)$; (d) $\theta_X(\omega)$; (e) $\theta_Y(\omega)$; (f) $\theta_Z(\omega)$. Key: ——, analytical (modal expansion method); ×, numerical (direct inversion method).

they are strictly determined by the passive path(s) of an active mount. The effect of active mount's orientation

angle, ϕ as shown in Fig. 6, on the focalized mounting system motions is also investigated here. Figure 10 compares the frequency responses in the roll direction for two different orientation angles given $T(t) = T_{eng} e^{j\omega t}$ with $T_{eng} = 100$ N m. The roll motion (θ_X) is significantly reduced in overall frequency range when $\phi = 0°$ (vertical) compared to the case with $\phi = 30°$. This shows that the orientation of the active mount plays important role in response reduction by active mount.

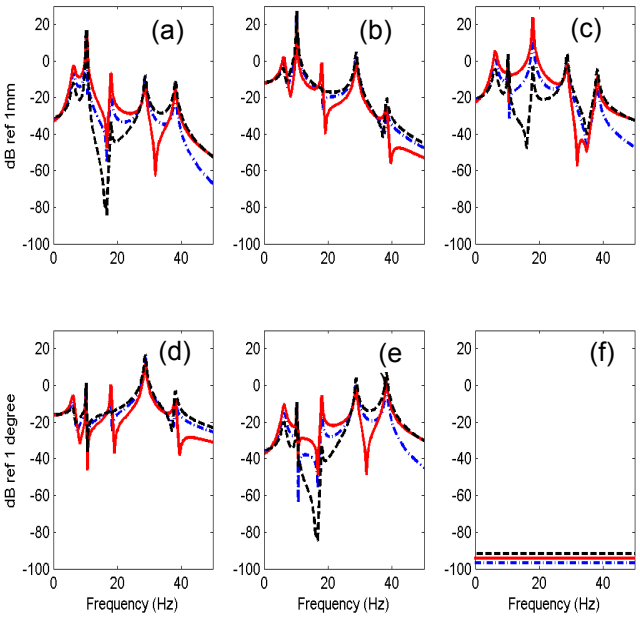

Fig. 9 Effect of active displacements on frequency responses of the active powertrain system (Fig. 6) given harmonic torque excitation with 100 Nm amplitude. One active mount of Fig. 5 is placed at location # 1 with an orientation angle $\phi = 0°$. (a) $X(\omega)$; (b) $Y(\omega)$; (c) $Z(\omega)$; (d) $\theta_X(\omega)$; (e) $\theta_Y(\omega)$; (f) $\theta_Z(\omega)$. Key: —·—, $X_A = 0mm$; — —, $X_A = 1.0mm$ with $\phi_A = 0°$; ——, $X_A = 1.5mm$ with $\phi_A = 180°$.

The torque roll axis (TRA) could be decoupled for a proportionally or non-proportionally damped system by judiciously selecting mount parameters, locations, orientation angles, and stiffness ratios as suggested by Jeong and Singh [2] and more recently Park and Singh [3]. Even though significant coupling takes place when spectrally-varying mounts are employed, decoupling is still possible for a focalized mounting system (with $\phi = 0°$ and $r_z = 0$ mm). Now, an active mount and a passive hydraulic mount are placed at location #1 and #2, respectively, for the focalized system (Fig. 6). To begin with, assume that active force is not applied under

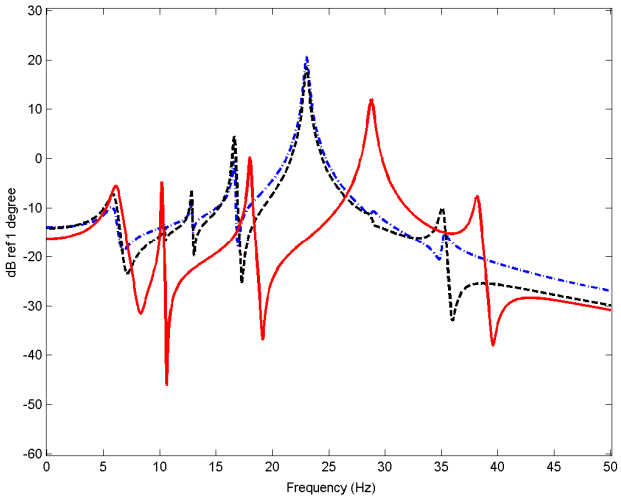

Fig. 10 Effect of orientation angle on frequency responses in roll direction ($\theta_X(\omega)$) of the active powertrain system (Fig. 6) given harmonic torque excitation with 100 Nm amplitude. One active mount of Fig. 5 is placed at location #1. Key: —·—, $X_A = 0mm$, $\phi = 30°$; — —, $X_A = 1.5mm$ with $\phi_A = 180°$, $\phi = 30°$; ——, $X_A = 1.5mm$ with $\phi_A = 180°$, $\phi = 0°$ (vertical).

the torque excitation. The TRA is decoupled given $\phi = 0°$ and $r_z = 0$ mm. Mount locations are illustrated in Fig. 11; and, Fig. 12 shows the resulting decoupled roll mode ($\theta_X(\omega)$). Next apply the active force; the roll mode is now coupled with $Z(\omega)$ and $\theta_Y(\omega)$. This is expected since the secondary force arising from the active mount introduces three excitations in $Z(\omega)$, $\theta_X(\omega)$, and $\theta_Y(\omega)$ in addition to the primary engine torque. This example clearly shows that one should carefully design the TRA mounting scheme while including the results of secondary forces generated by the active mount.

CONCLUSION

In this article, two methods for representing mounts with $k(\omega)$ and $c(\omega)$ are critically examined in describing the eigensolutions and frequency responses of an isolation system. To overcome the deficiencies of Method I (limited to only the frequency domain analysis), Method II is developed by employing transfer function (in Laplace domain). The analytical method compares well with the direct inversion method in predicting the frequency responses. Two major contributions emerge. First, a new 6-DOF rigid body model with a combination of active and passive mounts is proposed. To facilitate this development, a refined transfer function model for

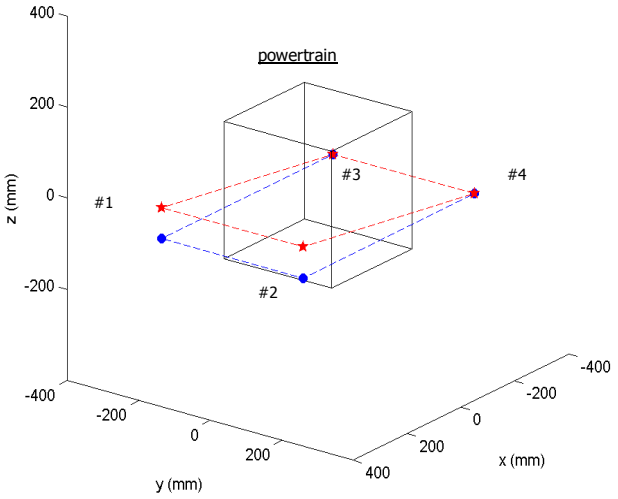

Fig. 11 Mount locations for coupled and decoupled powertrain of Fig. 6 given harmonic torque excitation. One active mount (with inactive actuator) of Fig. 5 is placed at location #1 and the rest are passive mounts; motions are decoupled by adjusting location and orientation angle of mount #1. Key: □, TRA decoupled ($\phi = 0°$, $r_z = 0mm$); ●, Coupled ($\phi = 15°$, $r_z = -68mm$)

fluid-piston displacement type active mounts is developed and then is incorporated into mounting system, resulting in a spectrally-varying linear time-invariant system formulation. Our model is partially verified by comparison with numerically obtained frequency response functions; also, complex eigensolutions match with measured natural frequencies for one powertrain example. Second, eigenstructure and multi-dimensional dynamics (especially motion coupling issues when excited by harmonic torque) are examined. For instance, modal solutions (that are dictated by the passive paths) are predicted as well as the role of active path. The effect of mount parameters such as orientation angle and location on motion decoupling is examined and appropriate selection of the passive path within active mount provides the torque roll axis decoupling. Coupling phenomena are illustrated by comparing powertrain motion spectra with and without operation of active mounts. The motion coupling issues introduced by the active mounts are explained via frequency responses. Future work includes extension of this work to other active isolation systems. Further, properties of an active mount could be specified from the system perspective (say decoupled motions, resonance control and reduced transmissibility) and then passive and active paths could be optimized to yield the desired performance over the frequency range of interest.

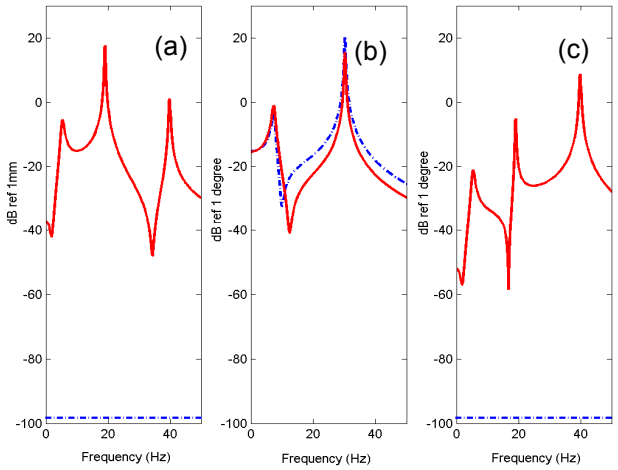

Fig. 12 Effect of active displacement on frequency responses of a decoupled powertrain of Fig. 6 given harmonic torque excitation with $100\ \mathrm{Nm}$ amplitude. One active mount of Fig. 5 is placed at location # 1 with an orientation angle $\phi = 0°$ and the actuator operates sinusoidally with different values of amplitude X_A and phase ϕ_A. (a) $Z(\omega)$; (b) $\theta_X(\omega)$; (c) $\theta_Y(\omega)$; other responses (not shown), $X(\omega)$ = $Y(\omega)$ = $\theta_Z(\omega)$ = 0. Key: — · —, $X_A = 0mm$; ——, $X_A = 1.5mm$ with ϕ_A = 180°. Observe coupling in $Z(\omega)$ and $\theta_Y(\omega)$ with $X_A = 1.5mm$ with ϕ_A = 180°

ACKNOWLEDGMENTS

We are grateful to the member organizations of the Smart Vehicle Concepts Center (www.SmartVehicleCenter.org) and the National Science Foundation Industry/University Cooperative Research Centers program (www.nsf.gov/eng/iip/iucrc) for supporting this work.

REFERENCES

1. C.M. Harris, *Shock and Vibration Handbook*, McGraw-Hill, New York, 1995 (Chapter 3).
2. T. Jeong and R. Singh, "Analytical methods of decoupling the automotive engine torque roll axis", *Journal of Sound and Vibration* 234, 85-114, (2000).
3. J. Park and R. Singh, "Effect of non-proportional damping on the torque roll axis decoupling of an engine mounting system", *Journal of Sound and Vibration* 313, 841-857, (2008).
4. H. Ashrafiuon, "Design optimization of aircraft engine mount Systems", *ASME Journal of Vibration and Acoustics* 115(4), 463-467, (1993).
5. H. Ashrafiuon and C. Nataraj, "Dynamic analysis of engine-mount systems", *ASME Journal of Vibration and Acoustics* 14(1), 79-83, (1992).

6. C.E. Spiekermann, C.J. Radcliffe, and E.D. Goodman, “Optimal design and simulation of vibrational isolation systems”, *Journal of Mechanisms Transmissions and Automation in Design* 107, 271-276, (1985).
7. J.S. Tao, G.R. Liu, and K.Y. Lam, “Design optimization of marine engine-mount system”, *Journal of Sound and Vibration* 235, 477-494, (2000).
8. R. Singh, G. Kim, and P.V. Ravindra, “Linear analysis of automotive hydro-mechanical mount with emphasis on decoupler characteristics”, *Journal of Sound and Vibration* 158, 219-243, (1992).
9. M.L. Tinker and M. A. Cutchins, “Instabilities in a non-linear model of a passive damper”, *Journal of Sound and Vibration* 176, 415-428, (1994).
10. E.I. Rivin, *Passive Vibration Isolation*, ASME Press, New York, 2003.
11. R.A. Ibrahim, “Recent advances in nonlinear passive vibration isolators”, *Journal of Sound and Vibration* 314 , 371-452, (2008).
12. Y. Yu, N.G. Naganathan, and R.V. Dukkipati, “Review of automotive vehicle engine mounting systems”, *International Journal of Vehicle Design* 24(4), 299-319, (2000).
13. S. He and R. Singh, “Estimation of amplitude and frequency dependent parameters of hydraulic engine mount given limited dynamic stiffness measurements”, *Noise Control Engineering Journal* 53(6), 271-285, (2005).
14. T. Jeong and R. Singh, “Inclusion of measured frequency- and amplitude-dependent mount properties in vehicle or machinery models”, *Journal of Sound and Vibration* 245, 385-415, (2001).
15. Y-W Lee and C-W Lee, “Dynamic analysis and control of an active engine mount system”, *Proc. Institution of Mech. Engineers, Part D: Journal of Automobile Eng.* **216**, 921-931, (2002).
16. T. Shibayama, K. Ito, T. Gami, T. Oku, Z. Nakajima, and A. Ichikawa, “Active engine mount for a large amplitude of idling vibration”, *SAE*, Paper #951298, (1995).
17. A. Gennesseaux, “A new generation of engine mounts”, *SAE*, Paper #951296, (1995).
18. K. Aoki, T. Shikata, Y. Hyoudou, T. Hirade, and T. Aihara, “Application of an active control mount (AEM) for improved diesel engine vehicle quietness”, *SAE*, Paper #1999-01-0832, (1999).
19. H. Matsuoka, T. Mikasa, and H. Nemoto, “NV countermeasure Technology for a cylinder-on-demand engine – Development of active control engine mount”, *SAE*, Paper #2004-01-0413, (2004).
20. P. Gardonio, S.J. Elliott, and R.J. Pinnington, “Active isolation of structural vibration on multi-degree-of-freedom system, part 1: the dynamics of the system”, *Journal of Sound and Vibration*, **207**, 61-93, (1997).
21. J-H Kim and C-W Lee, “Semi-active damping control of suspension systems for specified operational response mode”, *Journal of Sound and Vibration*, **260**, 307-328, (2003).
22. T.J. Royston and R. Singh, “Optimization of passive and active non-linear vibration mounting systems based on vibratory power transmission”, *Journal of Sound and Vibration*, **194**, 295-316, (1996).
23. A.J. Hillis, A.J.L. Harrison, and D.P. Stoten, “A comparison of two adaptive algorithms for the control of active engine mounts”, *Journal of Sound and Vibration*, **286**, 37-54, (2005).
24. Y. Nakaji, S. Satoh, T. Kimura, T. Hamabe, Y. Akatsu, and H. Kawajoe, “Development of active control engine mount system”, *Vehicle System Dynamics*, **32**, 185-198, (1999).
25. G. Kim and R. Singh, “A study of passive and adaptive hydraulic engine mount systems with emphasis on non-linear characteristics”, *Journal of Sound and Vibration*, **179**, 427-453, (1995).
26. A. Gennesseaux, “Research for new vibration isolation techniques: From hydro-mounts to active mounts”, *SAE*, Paper #931324, (1993).

CONTACT

Professor Rajendra Singh
Acoustics and Dynamics Laboratory
NSF I/UCRC Smart Vehicle Concepts Center
The Ohio State University
Email: singh.3@osu.edu
Phone: 614-292-9044
Website: www.AutoNVH.org